ABSTRACT

We describe an effort to map lesion to behavior by studying the comprehension of complex VP-Ellipsis constructions (e.g., The policeman defended the child, and the dedicated fireman did___ too…) in participants with Broca's aphasia. We quantified the lesions of our individual participants using cytoarchitectonic probability maps of the human brain. We found that our Broca participants evinced delayed priming of the object in the ellipsis clause, while off-line comprehension was largely spared. Structure-function analyses revealed that lesions in both temporal and frontal areas participated in the behavioral outcomes, though each region seems to have played a distinct role.

We describe a novel exploration into receptive abilities of brain-damaged individuals with aphasia, and its relation to their lesions. **Behaviorally**, we investigate the comprehension of verb phrase ellipsis (VPE) – a complex sentence type that has rarely been studied in aphasia, yet shares important properties with constructions that are known to be impaired. We investigate this construction from both on- and off-line perspectives in the same patients. **Anatomically**, we obtain a quantitative picture of patients' lesions by mapping them onto a probabilistic cytoarchitectonic map that parses the human brain into functionally coherent parts. Finally, we investigate the relation between lesion anatomy and behavior in predicting individual variation in aphasia.

Verb phrase ellipsis is a bi-clausal syntactic construction where most of the VP is missing in the second clause, relying on the first for its interpretation, e.g., "The policeman defended the child, and the fireman did__too" (meaning: 'The fireman defended the child too'). The missing VP leaves a 'gap' following the bare auxiliary *did*, of which the VP of the first clause is antecedent (Johnson, 2001). As a receptive deficit for other gap-containing sentences is well documented in aphasia, both off- and on-line (Grodzinsky, 1986, 2000; Love et al., 2008; Poirier et al., 2009; Shapiro et al., 1998), we inquired whether this deficit extends to VPE.

Methods

Participants (Table 1). Seven adults with agrammatic aphasia participated in the study. All had experienced a single, unilateral left hemisphere stroke. Diagnosis of agrammatism was based on the BDAE (version 3; Goodglass, Kaplan, & Barresi, 2000), and the WAB (Kertesz, 2006). Comprehension deficits were defined as chance performance comprehension of non-canonical (object-relative and passive) sentences from the SOAP Test (Love & Oster, 2002).

Materials and Design

Off-line task. Ninety action-depicting sentences with VPE (e.g., the girl kicked a tiger and the boy did __ too) were presented aurally, along with one token of 4 types of pictures ("Match" and 3 "MisMatches") in a Truth-Value-Judgment Task. 45 sentences with 2 conjoined full clauses (e.g., the girl kicked a tiger and the boy kicked a tiger) served as controls.

On-line task. We created 40 experimental sentences with VPE, as in (1).

(1) The policeman defended the child, and the dedicated [PP0] fireman did___ [PP1] too, according [PP2] to people at the scene.

In (1), the ellipsis phrase (__) refers to the overt VP (*defended the child*). We tested for activation of the object NP from the first clause (e.g., *the child*) that is elided in the second clause, at three positions: a baseline test point [PP0] 750 ms before the ellipsis phrase, the ellipsis phrase [PP1], and a downstream test point [PP2] 750 ms after PP1. Activation of the object NP is

expected at [PP1] for unimpaired comprehenders. Patients with comprehension deficits may be delayed until [PP2] (Love et al., 2008). Eighty filler sentences were also included.

Procedure. For the cross-modal priming (CMP) task, participants listened to uninterrupted sentences for comprehension and simultaneously made a binary button-press decision (Human/Not-Human) to a brief computer-presented picture probe that appeared during the sentence. Participants were asked comprehension questions throughout the experiment to ensure they were attending. In addition, high-resolution anatomical MR images were acquired for each participant.

Data Analysis

CMP Analysis: Response times (RTs) for the group were analyzed using a mixed-effects regression model with crossed random effects of Participant and Sentence, and fixed effects of Probe Position (PP0 vs. PP1 vs. PP2), Relatedness (Related vs. Control), and their interaction. We focus on *t*-statistics for *a priori* planned comparisons of Related and Control probes at each probe position; *p*-values are reported two-tailed.

Structural Analysis: Using AFNI (Cox, 1996), whole brain and lesion masks were created for participants. Probabilistic maps of cytoarchitectonic areas belonging to the Jülich Brain Mapping Project (Amunts et al., 1999; Zilles & Amunts, 2010) were transformed on each participant's brain based on non-linear registration (Hömke et al., 2009). The registration was restricted by masking the lesion. Each voxel from the anatomical scan was assigned a probability of belonging to a particular anatomical region. Thus for each participant we computed the proportion of lesioned tissue with respect to a cytoarchitectonic area. We defined two left hemispheric regions of interest (ROI). The first was in inferior frontal gyrus (IFG), covering Brodmann's areas BA44 and BA45 (roughly, Broca's area). The second ROI was in the temporal lobe, and corresponded to the area covered by superior temporal gyrus, middle temporal gyrus, and Wernicke's area (TE3; Morosan et al., 2005). We chose these two broad regions as they have been implicated in comprehension deficits in aphasia.

Structure-Function Correspondence. We computed point-biserial correlations for each participant at each test point: Probes were recoded as 0 (related) or 1 (control) for each response and correlated with response times using a standard Pearson correlation. The resulting r-value is an effect size, with values ranging from -1 (inhibition) to 1 (priming). The r-values were used as the dependent variable in a least-squares regression analysis with the proportion of lesioned tissue in each of our two ROIs as independent variables.

Results and Discussion

Overall, *patients evinced delayed on-line processing with spared off-line comprehension.* As a group, the patients showed no priming for the direct object at baseline or at the ellipsis position, but did show a significant priming effect downstream (at PP2) (Table 2). In the off-line sentence-

picture matching test of final comprehension, patients had above-chance comprehension on all conditions, and were spared on the matched ellipsis condition, with 95% accuracy.

Results from the structure-function analyses revealed a nuanced pattern across individual participants (Table 3; Figure 1). Both ROIs played a role in the time-course of priming effects. At the ellipsis phrase (PP1), greater temporal damage resulted in smaller priming effects. In contrast, greater damage to IFG resulted in larger priming effects. The opposing directions of the effects suggest that these two regions play different functional roles. The reduction of priming with temporal lobe damage suggests that the temporal lobe is the source of the priming effects. Increased priming with IFG damage suggests that IFG plays a modulatory role.

Furthermore, this pattern holds for the change in priming between the ellipsis phrase and PP2, where this structure-function pattern is no longer observable. That is, relatively smaller temporal lobe lesions results in on-time priming at PP1 and a decay in activation at PP2, whereas relatively larger temporal lobe lesions results in delayed priming, which only emerges at PP2. The null finding at PP2 likely reflects the confluence of decayed on-time priming and emergent delayed priming.

Thus the delayed priming effect for the group average data appeared to be driven by participants with relatively larger temporal lobe than IFG lesions.

The contrast between spared comprehension and the on-line deficit is puzzling: the former indicates that VPE falls outside the scope of the syntactic movement deficit typical of Broca's aphasia (Grodzinsky, 1986; 2000); however the on-line deficiency is reminiscent of the deficit observed in standard filler-gap constructions in Broca's aphasia. In the presentation, we will consider possible explanations for this apparent paradox, and pay special attention to the significance of the structure-function correspondence we discovered, and the way it reflects the joint activity of multiple cortical regions.

References

Amunts, K. Axel Schleicher, Uli Bürgel, Hartmut Mohlberg, Harry B.M. Uylings, and Karl Zilles. (1999). Broca's region revisited: Cytoarchitecture and intersubject variability. *Journal of Comparative Neurology*, 412, 319–341.

Cox, R.W. (1996). AFNI: software for analysis and visualization of functional magnetic resonance neuroimages. *Computers and Biomedical Research*, 29, 162–173.

Goodglass, H., Kaplan, E., & Barresi, B. (2000). *Boston diagnostic aphasia examination (3rd Ed.)*. Philadelphia: Taylor & Francis.

Grodzinsky, Yosef. (1986). Language deficits and the theory of syntax. *Brain & Language, 27*. 135-159.

Grodzinsky, Yosef. (2000). The neurology of syntax: language use in the absence of Broca's area. *Behavioral & Brain Sciences, 20*, 1-71.

Hömke, L., Amunts, K., Bönig, L., Fretz, C., Binkofski, F., Zilles, K., Weder, B. (2009). Analysis of lesions in patients with unilateral tactile agnosia using cytoarchitectonic probabilistic maps. *Human Brain Mapping* 30:1444-1456.

Johnson, Kyle. (2001). "What VP ellipsis can do, what it can't, but not why," in The handbook of contemporary syntactic theory, Mark Baltin and Chris Collins (eds.) Blackwell Publishers, pp. 439-479.

Kertesz, A. (2006). *Western aphasia battery (Revised).* San Antonio: PsychCorp.

Love, T., & Oster, E. (2002). On the categorization of aphasic typologies: The SOAP (a test of syntactic complexity). *Journal of Psycholinguistic Research, 31*(5), 503–529.

Love, T., Swinney, D. Walenski, M. and Zurif, E. (2008). How left inferior frontal cortex participates in syntactic processing: evidence from aphasia. Brain and Language, *107, 203–219.*

Morosan, P., Schleicher, A., Amunts, K., Zilles, K. (2005). Multimodal architectonic mapping of human superior temporal gyrus. Anatomy and Embryology, 210(5-6), 401-406.

Poirier, J., Shapiro, L., Love, T., Grodzinsky, Y. (2009). The On-line Processing of Verb-phrase Ellipsis in Aphasia. *Journal of Psycholinguistic Research, 38 (3), 237-254.*

Shapiro, L., Swinney, D., and Borsky, S. (1998) Online Examination of Language Performance in Normal and Neurologically Impaired Adults. *American Journal of Speech-Language Pathology*. 7: 49-60.

Zilles, K, and Amunts, K. (2010). Centenary of Brodmann's map--conception and fate. *Nature Reviews Neuroscience, 11(2)*, 139-45.

TABLES AND FIGURES

Table 1. Demographic and lesion information for participants with aphasia.

Patient	BDAE[a] Severity	WAB[b] Aphasia Quotient	SOAP[c] Canonical	SOAP[c] Non-canonical	Gender	Age at Testing	Time Post Stroke	Education	Lesion location[d]
LHD004	4	92.4	95%	50%	M	68;2	11;11	8th grade	L IFG extending into the basal-ganglia, internal capsule, lenticular nucleus.
LHD009	3	76.3	75%	55%	M	59;11	11;7	5 yrs college	Large L lesion involving inferior frontal gyrus (BA 44,45) .
LHD019	1	54.1	90%	20%	F	60;2	15;1	High School	L MCA embolic stroke; distribution encompasses broad left frontal lobe region.
LHD040	2	76.7	60%	60%	M	61;1	5;4	B.A.	Small L subcortical lesion involving the Basal Ganglia.
LHD101	2	82.4	95%	35%	M	60;10	4;5	PhD	Large L lesion involving posterior inferior frontal gyrus (BA44) with posterior extension.
LHD130	4	81.1	95%	65%	M	57;3	1;9	B.A.	L IPL with posterior extension sparing of Wernicke's area, but more inferior temporal involvement .
LHD132	4	81.9	70%	75%	M	46;8	5;4	B.A.	Large L lesion primarily involving the Insula (with small extension to Broca's area and posterior extension involving the temporal lobe).

[a] BDAE = Boston Diagnostic Aphasia Examination

[b] Western Aphasia Battery

[c] Subject-relative, Object-relative, Active and Passive. The canonical score is the mean percent correct of the active and subject relative sentences; the non-canonical score is the mean percent correct of the passive and object relative sentences.

[d] L = left; MCA = middle cerebral artery; IPL = inferior parietal lobule; STG = superior temporal gyrus

Table 2. Group-average mean response time (and standard error) in milliseconds for control and related probes and priming effects at each probe position.

	Control	Related	Priming Effect (control – related)	Significance
Baseline (PP0)	942 (18)	929 (19)	13	$t(223)=0.55$, $p=0.58$
Ellipsis Site (PP1)	893 (16)	900 (17)	-7	$t(222)=0.00$, $p=0.99$
Downstream (PP2)	916 (19)	880 (16)	36	$t(234)=2.22$, $p=0.03$

Table 3. Results from the regression models testing correspondences between lesion regions of interest (ROI) and priming effect sizes at each test point and for the change in priming across test points.

Test Point	ROI[a]	Coefficient (B)	Significance (*p*)	Model R^2
Baseline (PP0)	IFG	0.05	0.76	0.16
	TEMP	-0.13	0.44	
Change from baseline to ellipsis (PP1 – PP0)	IFG	0.42	0.14	0.71
	TEMP	-0.73	0.04	
Ellipsis Phrase (PP1)	IFG	0.46	0.01	0.94
	TEMP	-0.87	0.002	
Change from ellipsis to downstream (PP2 – PP1)	IFG	-0.35	0.03	0.95
	TEMP	1.01	0.0009	
Downstream (PP2)	IFG	0.11	0.4	0.49
	TEMP	0.14	0.33	

[a] IFG = inferior frontal gyrus (BA44 + BA45); TEMP = temporal lobe (superior temporal gyrus + middle temporal gyrus + TE3)

Figure Captions

Figure 1. (a) Priming effects (y-axis; note that the values have been linearly transformed to match the range of the x-axis values) at the ellipsis phrase (PP1), plotted against the proportion of lesioned tissue (x-axis) in IFG (open circle) and TEMP (filled circle). The solid lines connect the regions from each patient. The pattern of a positive effect for a lesion in Broca's area (more damage = more priming) and a negative effect for a temporal cortical lesion (more damage = less priming) can be seen. (b) Priming effects are plotted against the difference of IFG and TEMP (IFG-TEMP). This more clearly shows that when IFG is more damaged than TEMP (positive value on the x-axis), larger priming effects obtain, and when TEMP is more damaged than IFG (negative values on the x-axis), smaller priming effects are found. This difference score significantly predicts priming ($B=0.64$, $p=0.01$, $r^2=0.75$).

Figure 1.

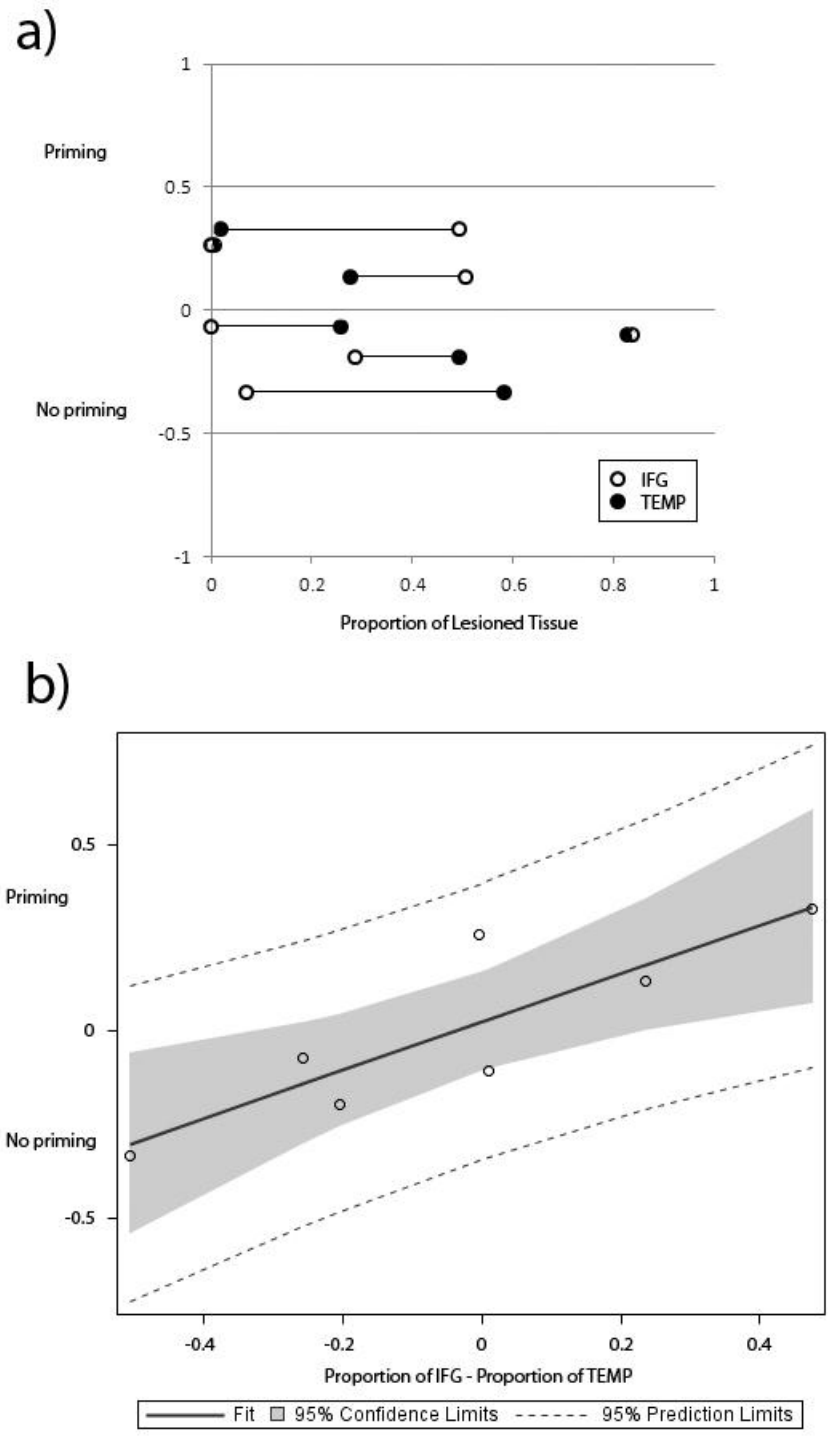
a)
Priming
No priming
1
0.5
0
-0.5
-1
0
0.2
0.4
0.6
0.8
1
Proportion of Lesioned Tissue
IFG
TEMP
b)
Priming
No priming
0.5
0
-0.5
-0.4
-0.2
0
0.2
0.4
Proportion of IFG - Proportion of TEMP
Fit
95% Confidence Limits
95% Prediction Limits